Journal of Orthopaedic Surgery and Research

RESEARCH

Open Access

Modeling and construction of nomogram of cage subsidence after single-segment transforaminal lumbar interbody fusions

Jinxiang Zhan[1,2†], Qipeng Wei[1*†], Weijun Guo[1], Zihao Liu[2], Shiji Chen[2], Qingyan Huang[1] and Dongling Cai[1*]

Abstract

Objective The purpose of this study is to explore and analyze the risk factors for interbody cage subsidence in patients undergoing single-segment transforaminal lumbar interbody fusion (TLIF) and to construct and validate a visual nomogram risk prediction model.

Methods A retrospective analysis was conducted on the clinical data of 159 patients who underwent single-segment TLIF at the Spine Surgery Department of Panyu District Traditional Chinese Medicine Hospital from January 2021 to June 2023. Using the caret package in R, patients were randomly divided into a training set ($n=111$) and a validation set ($n=48$) in a 7:3 ratio. Multivariable logistic regression was employed for variable selection and the construction of the nomogram model. The predictive model's discrimination, calibration, and clinical utility were evaluated using receiver operating characteristic (ROC) curves, calibration curves, and decision curve analysis (DCA).

Results There were no statistically significant differences in various indicators between the training set ($n=111$) and the validation set ($n=48$) ($P>0.05$). Univariate analysis in the training set revealed that age, bone density, endplate morphology, anterior vertebral bone spurs, lumbar CT values, and VBQ were statistically significant. Multivariable logistic regression analysis indicated that bone density, anterior vertebral bone spurs, and lumbar CT values were independent predictors of interbody cage subsidence ($P<0.05$), and a nomogram model was constructed based on these indicators. The area under the ROC curve (AUC) for the training set and validation set was 0.93 (95% CI 0.89–0.98) and 0.93 (95% CI 0.86–1.00), respectively. The calibration curves showed good fit (training set $P=0.616$; validation set $P=0.904$). DCA analysis demonstrated that the model has high clinical utility.

Conclusion Bone density, anterior vertebral bone spurs, and lumbar CT values are risk factors for interbody cage subsidence in patients after single-segment transforaminal lumbar interbody fusion. The constructed nomogram model exhibits good predictive value and clinical utility.

†Jinxiang Zhan, Qipeng Wei contributed equally to this work.

*Correspondence:
Qipeng Wei
qipeng_wei@126.com
Dongling Cai
cdl_spine@126.com

Full list of author information is available at the end of the article

Keywords Transforaminal lumbar interbody fusion, Cage subsidence, Risk factor analysis, Nomogram, Predictive modeling

Lumbar degenerative changes refer to the accelerated aging process of the lumbar spine due to increasing age, excessive activity, and overload [1]. Under external forces, pathological changes may occur in the lumbar spine, leading to the rupture of the annulus fibrosus and herniation of the nucleus pulposus, which can result in low back pain and neurological dysfunction [2]. According to the "China Degenerative Spine Health Report 2023", the population affected by lumbar diseases in China has reached 200 million, with an incidence rate of 80% among adults. Furthermore, as the elderly population in China rapidly increases, the incidence of lumbar degenerative diseases is also rising year by year [3]. Lumbar interbody fusion surgery is an important method for treating lumbar degenerative diseases, and it typically yields good therapeutic outcomes, significantly alleviating patients' pain and improving their quality of life.

Lumbar interbody fusion surgery is an effective treatment for lumbar diseases; however, this procedure may also lead to certain complications. Among these, interbody cage subsidence is one of the most common complications. Recent literature indicates that the incidence of interbody cage subsidence after posterior lumbar fusion ranges from 26–50% [4, 5]. When subsidence occurs, the interbody device may migrate into the endplate or cancellous bone, reducing intervertebral height. This can lead to various issues, including failure of internal fixation, formation of a pseudarthrosis, kyphotic deformity, adjacent segment disease, and decreased foraminal height. Any of these conditions may trigger recurrent nerve root impingement and radicular pain [6–8].

Recent studies have revealed various risk factors associated with interbody cage subsidence. These factors include older age, smoking, higher body mass index (BMI), low bone density, excessive correction of intervertebral height, low lumbar CT values, as well as higher vertebral bone quality scores and endplate bone quality scores [9–14]. Although multiple methods exist for assessing postoperative risk, their accuracy and practicality still require improvement. Therefore, this study aims to analyze the risk factors for interbody cage subsidence following single-segment transforaminal lumbar interbody fusion and to establish a visual nomogram prediction model. By constructing this nomogram prediction model, we hope to provide clinicians with a more precise preoperative assessment tool, thereby optimizing patient treatment plans and reducing the incidence of postoperative complications.

Materials and methods

General information

This study retrospectively analysed 159 patients who underwent single-segment transforaminal lumbar interbody fusion at the Department of Spine Surgery, Panyu District Hospital of Traditional Chinese Medicine between January 2021 and June 2023. The procedures were performed by the same group of senior spine surgeons at the Panyu District Hospital of Traditional Chinese Medicine in Guangzhou, China, and the implants used were PEEK cages designed to provide optimal stability and support for spinal fusion. The technical specifications of the cage included PEEK. In this study, all patients received a PEEK cage replacement during surgery. Patients were randomised 7:3 into a training set ($n = 111$) and a validation set ($n = 48$) using the R language caret package. The training and validation sets were categorized based on the degree of interbody cage subsidence into a non-subsidence group (subsidence < 2 mm) and a subsidence group (subsidence ≥ 2 mm).

Inclusion criteria were as follows: [1] Patients must have undergone single-segment transforaminal lumbar interbody fusion at our hospital, with complete preoperative lumbar X-ray, CT, and MRI data; [2] Follow-up duration must exceed 12 months, with follow-up data including lumbar X-ray or CT; [3] Patients must have symptomatic lumbar degenerative diseases (such as lumbar spinal stenosis, lumbar spondylolisthesis, or others) that showed no improvement after at least 3 months of conservative treatment; [4] MRI and CT results must be consistent with clinical symptoms.

Exclusion criteria included: [1] Patients who had previously undergone lumbar fusion surgery; [2] Patients with comorbid conditions such as diffuse idiopathic skeletal hyperostosis, ankylosing spondylitis, lumbar infections, lumbar tumors, and lumbar trauma; [3] Patients with grade III or higher lumbar spondylolisthesis; [4] Patients for whom measurement was difficult due to Schmorl's nodes, local bone sclerosis, and interference artifacts; [5] Patients who experienced interbody cage subsidence at the first follow-up after discharge. This study was approved by the Ethics Committee of Panyu Traditional Chinese Medicine Hospital, and the use of retrospective data waived the requirement for individual consent.

Methods

General information

The purpose of this study is to collect and record the following demographic characteristics of the two groups of patients: age, sex, history of hypertension, history of

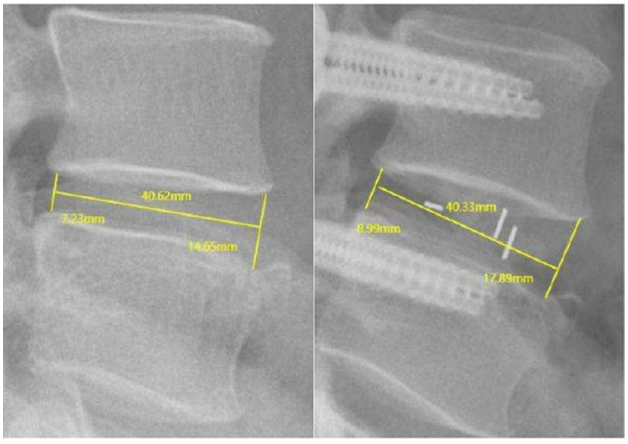

Fig. 1 Preoperative and postoperative lumbar DR showing the height of the anterior and posterior margins of the L4-5 intervertebral space and the measurement of the width of the sagittal plane

diabetes, smoking history, length of hospital stay, duration of surgery, surgical segment, intraoperative blood loss, body mass index (BMI), and bone density, in order to conduct relevant statistical analyses.

Imaging information

Measurement and evaluation of relevant parameters of preoperative and postoperative imaging of patients through PACS system:

1) The formula for calculating the Farfan index: (a + b)/c × 100%, where a is the height of the anterior edge of the intervertebral space, b is the height of the posterior edge of the intervertebral space, and c is the width of the intervertebral space in the sagittal plane.The corrected value of the Farfan index was calculated as follows: postoperative Farfan index - preoperative Farfan index (see Fig. 1).
2) Evaluation of endplate morphology: Select the median sagittal plane in the CT image and draw a line segment AB connecting the anterior edge of the endplate (point A) and the posterior edge of the endplate (point B), and then make a vertical line segment between AB and the endplate at a spacing of 1 mm, of which the longest vertical line segment is defined as CD, and the length of which is the endplate concavity depth (ECD). Three types of endplate morphology were defined according to the ECD as follows: flexed: ECD > 1 mm; flat: ECD ≤ 1 mm; and irregular: endplate localized beyond the plane of the anterior-posterior edge of the endplate (the ECD length of this type of endplate could not be measured). When the upper and lower endplates of the same disc segment have different morphologies, they are defined according to the principle of equivalence (e.g., if the upper endplate is flexed and the lower endplate is flat, the endplate morphology of the segment is defined as flat, see Fig. 2) [15, 16].
3) Methods of assessing the bony redundancy at the anterior margin of the vertebral body: combined with the patient's preoperative lumbar lateral DR images, the degree of bony redundancy at the anterior margin of the operated vertebral body was observed. According to the NATHAN classification criteria [17], the bone capillaries were divided into four grades: Grade I: isolated hyperplasia with increased density at the anterior margin of the vertebral body; Grade II: the bone capillaries were obviously protruding and were basically at the level of the endplates; Grade III: the bone capillaries were in the form of curved bird's beak and were close to the neighboring vertebrae: a bone bridge was formed between the neighboring vertebrae. Osteoid grades of III degree and above are considered as osteophyte formation at the anterior margin of the vertebral body (see Fig. 3) [18].
4) Measurement Method of CT Values for Lumbar Vertebrae: CT values are measurements obtained by computerised tomography and are used specifically

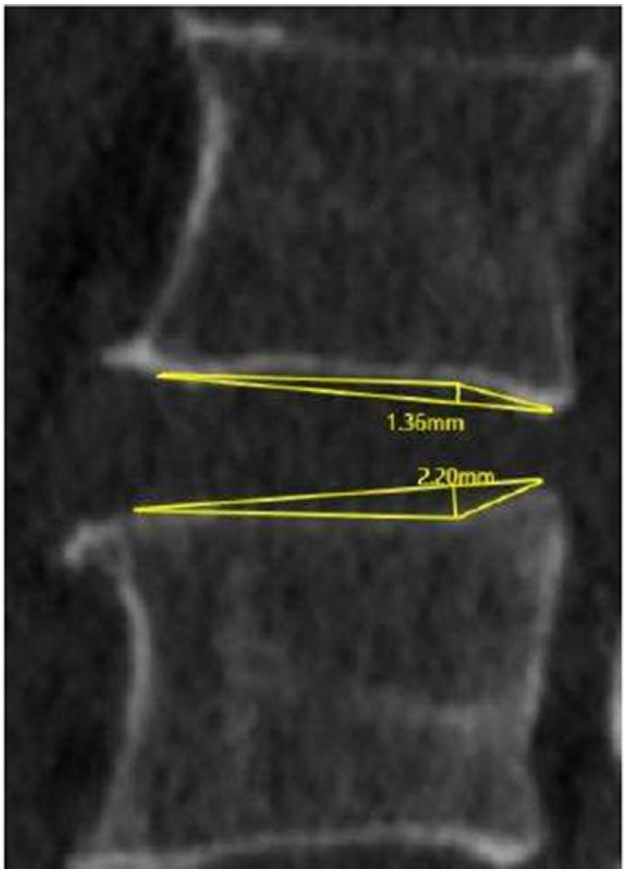

Fig. 2 Preoperative lumbar CT showing the measurement of endplate flexion depth at L4-5 segments

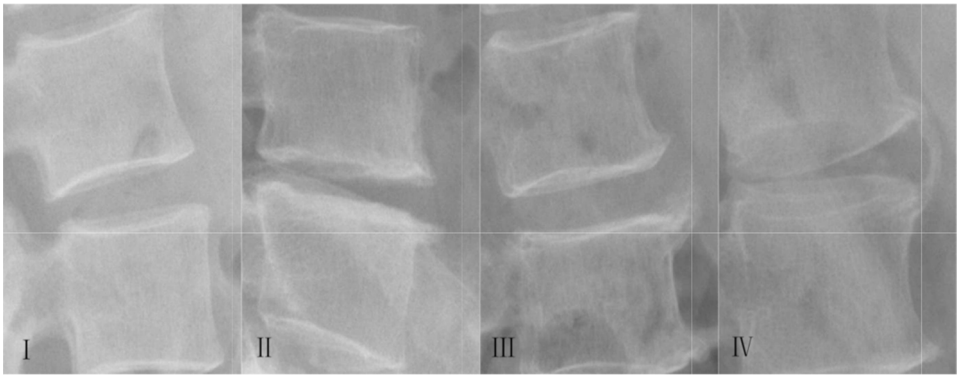

Fig. 3 Preoperative DR showing the degree of osteophyte proliferation at the anterior margin of L4-5 vertebral body-NATHAN classification criteria

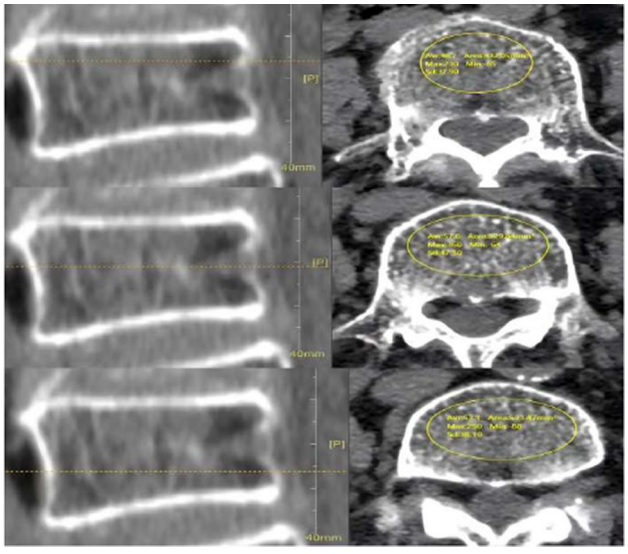

Fig. 4 Measurement of lumbar CT values. The figure illustrates the process of selecting a region of interest (ROI) within a single vertebral cancellous bone region, avoiding areas of cortical bone and degenerative structures. The average CT value within the ROI is automatically read by the viewing software

to assess the density of cancellous bone in the lumbar spine. These values are expressed in Hounsfield units (HU) and are important in assessing bone quality. CT images of vertebrae from L1 to L4 were selected for measurement, with the cancellous bone area at the center of the vertebral body as the region of interest (ROI). The ROI should avoid areas of cortical bone, local osteophyte formation, degenerative structures, and the venous plexus at the posterior part. The average CT value within the ROI was automatically read using viewing software (such as the PACS system) (see Fig. 4). For each vertebra (L1 to L4), CT values were measured at three levels: the layer just beneath the superior endplate, the middle layer of the vertebral body, and the layer just above the inferior endplate. The average CT value for each vertebra was then calculated to obtain the overall CT value for the lumbar spine [19].

5) VBQ Measurement Method: VBQ is a parameter used to assess vertebral bone quality. In the mid-sagittal T1-weighted MRI images, the region of interest (ROI) was defined as the cancellous bone area of the vertebral body from L1 to L4, as well as the cerebrospinal fluid (CSF) region at the level of L3. The average signal intensity within the ROI was measured and compared to the average signal intensity of the CSF at the L3 level. The VBQ score was then calculated as the ratio of the average signal intensity of the L1 to L4 vertebral bodies to that of the CSF at the L3 level (see Fig. 5) [20]. Both measurements were performed independently by two orthopedic surgeons who were unaware of the surgical outcomes. The average of their measurements was taken. If the difference between their scores exceeded 10%, a third author, who was also unaware of the surgical results, was consulted.

Statistical analysis

Data analysis was performed using R 4.3.2 and SPSS 27.0 statistical software. The significance level was set at $\alpha = 0.05$, and a p-value < 0.05 was considered statistically significant. For continuous variables with a normal distribution, independent samples t-test was used, with results expressed as mean ± standard deviation ($x \pm s$). For continuous variables with a non-normal distribution, the Mann-Whitney U test was employed, and the data were presented as median (25th percentile, 75th percentile) [M(P25, P75)]. Categorical variables were analyzed using chi-square test, Fisher's exact test, or non-parametric tests as appropriate. Variables that showed statistical significance between the fusion implant subsidence group and non-subsidence group in the training cohort were incorporated into a multivariable logistic regression model to identify predictors. A nomogram was subsequently developed based on the selected variables from the multivariable analysis to predict post-operative

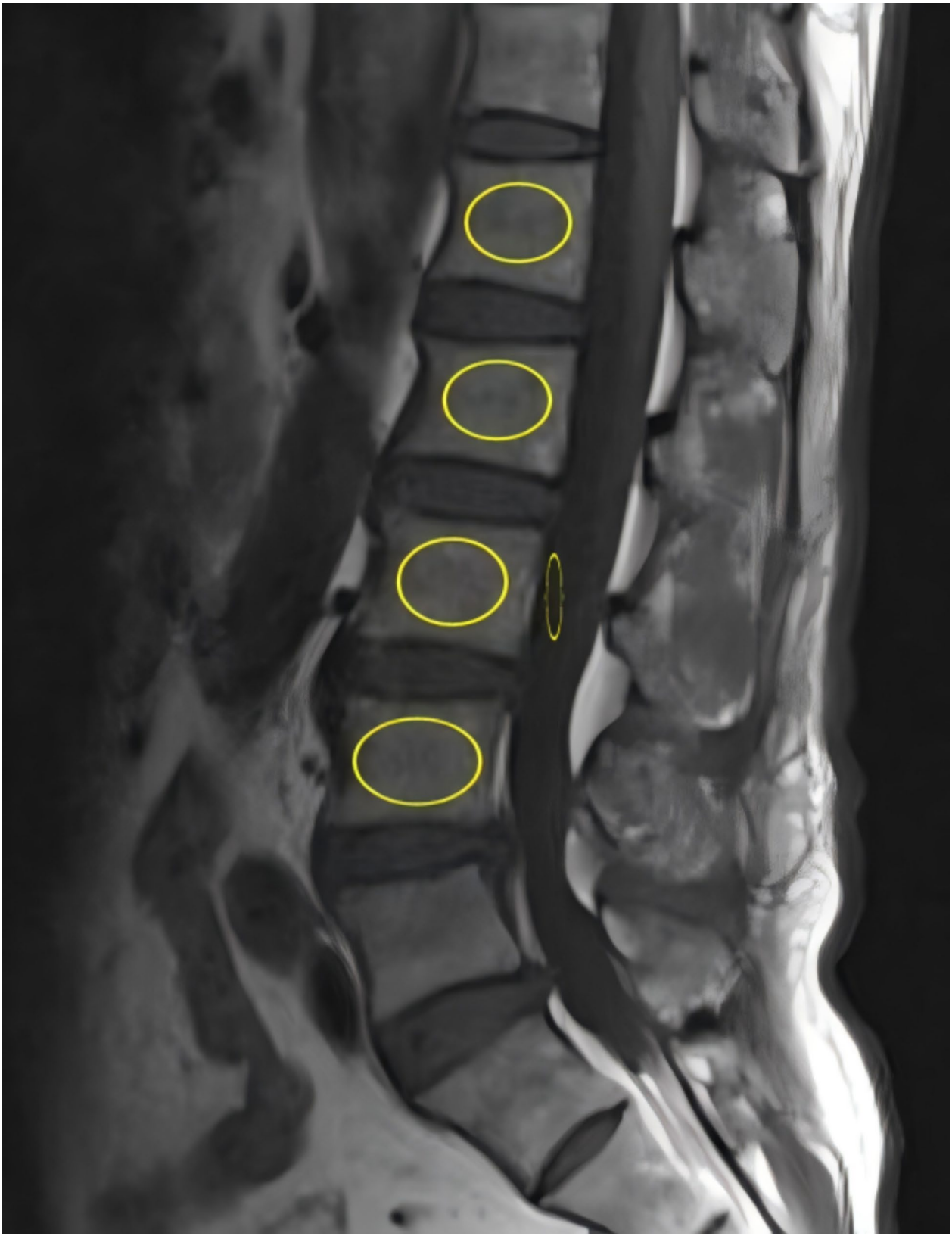

Fig. 5 VBQ measurements. This figure shows the calculation of the VBQ score, which is the ratio of the average signal intensity of the L1 to L4 vertebrae to the CSF signal intensity at the L3 level. This measurement is essential for assessing vertebral bone quality and its impact on surgical outcomes

Table 1 Comparative results of clinical data in the training and validation sets

Factor	Training Set (*n* = 111)	Validation Set (*n* = 48)	Statistic	*P*-value
Gender/Case			x2 = 0.016	0.900
Male	29(73.9%)	13(27.1%)		
Female	82(26.1%)	35(72.9%)		
Age (years)	65(56,72)	53.50(50.25, 59.00)	Z=-1.560	<0.001
Hypertension			x2 = 1.073	0.300
Yes	26(23.4%)	15(31.3%)		
No	85(76.6%)	33(68.8%)		
Diabetes			x2 = 3.687	0.055
Yes	11 (9.9%)	0 (0%)		
No	100(90.1%)	48(100%)		
Smoking			x2<0.001	1.000
Yes	4 (3.6%)	2 (4.2%)		
No	107(96.4%)	46(95.8%)		
Hospital Stay (days)	15.00(13.00, 17.00)	14.00(13.00, 17.75)	Z=-0.290	0.771
Surgery Duration (minutes)	180.00(150.00, 225.00)	180.00(151.25, 220.00)	Z=-0.101	0.919
Intraoperative Blood Loss (ml)	200(150, 400)	200(150, 300)	Z=-1.005	0.315
BMI (kg/m^2)	23.10(21.61, 24.65)	23.22(22.61, 24.91)	Z=-0.682	0.496
Bone Density	-2.10(-2.80, -1.20)	-2.15(-2.78, -1.30)	Z=-0.417	0.677
Preoperative Farfan Index	58.85% ± 10.64%	57.61% ± 9.53%	t = 157	0.487
Postoperative Farfan Index	69%(59%, 75%)	69%(62%, 75%)	Z=-0.550	0.582
Adjusted Farfan Index	9.5%(4.4%, 14.7%)	11.75%(7.00%, 15.95%)	Z=-1.538	0.124
Surgical Segment/Case			Z=-0.510	0.610
L2-3	0 (0%)	1 (2.1%)		
L3-4	1 (0.9%)	1 (2.1%)		
L4-5	78(70.3%)	33(68.7%)		
L5-S1	32(28.8%%)	13(27.1%)		
Anterior Vertebral Osteophyte			Z=-0.205	0.837
Grade 1	73(65.8%)	33(68.7%)		
Grade 2	27(24.3%)	9 (18.8%)		
Grade 3	10(9.0%)	5 (10.4%)		
Grade 4	1 (0.9%)	1 (2.1%)		
Endplate Morphology			Z=-1.211	0.226
Flat Type	35(31.5%)	22(45.8%)		
Concave Type	53(47.7%)	16(33.4%)		
Irregular Type	23(20.8%)	10(20.8%)		
Lumbar CT Value	124.99 ± 50.26	113.64 ± 38.38	t = 115.435	0.123
VBQ	2.92(2.64, 3.36)	2.85(2.45,3.27)	Z=-0.835	0.404

implant subsidence. The performance of the model was validated using receiver operating characteristic (ROC) curves, calibration curves, and the Hosmer-Lemeshow goodness-of-fit test. Additionally, the clinical utility of the model was assessed using decision curve analysis (DCA).

Results

Comparison of clinical data

In this study, 159 patients were randomly divided into two groups at a ratio of 7:3: the training cohort ($n = 111$) and the validation cohort ($n = 48$). No statistically significant differences were observed between the two groups in terms of demographic and clinical characteristics ($P > 0.05$) (see Table 1).

In the training cohort, significant differences were found between the fusion implant subsidence group and the non-subsidence group across multiple variables, including age, bone mineral density (BMD), endplate morphology, vertebral body anterior osteophytes, lumbar spine CT values, and VBQ scores. These differences were statistically significant ($P < 0.05$) (see Table 2). However, no significant differences were observed between the two groups regarding gender, history of hypertension, diabetes, smoking, length of hospital stay, operative time, surgical segment, intraoperative blood loss, body mass index (BMI), preoperative Farfan index, postoperative Farfan index, or Farfan index correction value ($P > 0.05$) (see Table 2).

Multivariate logistic regression model analysis

Based on the statistically significant factors identified in the univariate analysis of the training set, these factors were utilized as independent variables, while the occurrence of interbody fusion cage subsidence post-surgery was designated as the dependent variable for the multivariate logistic regression model analysis. The results indicated that bone density, anterior vertebral osteophytes, and lumbar CT values are independent predictors of interbody cage subsidence (see Table 3).

Model construction

Based on the results of the multivariate logistic regression model analysis, we constructed a nomogram incorporating bone density, anterior vertebral osteophytes, and lumbar CT values, with a total score of 280 points (see Fig. 6). For instance, consider a patient who underwent L4-5 single-segment transforaminal lumbar interbody fusion. This patient presented with a grade 2 anterior vertebral osteophyte, corresponding to a score of 65 points. The bone density was −2.5, which yielded a score of 60 points. The lumbar CT value was 80, corresponding to a score of 67 points. Summing these scores resulted in a total of 192 points, indicating a risk greater

Table 2 Comparative results of clinical data in the training set between the cage subsidence and Non-cage subsidence groups

Factor	Cage subsidence group($n=49$)	Non-cage subsidence group($n=62$)	Statistic	*P*-value
Gender/Case			$x^2=0.615$	0.433
Male	11(22.4%)	18(29.0%)		
Female	38(77.6%)	44(71.0%)		
Age (years)	65.00(54.00,71.00)	53.50(50.00, 60.00)	$Z=-4.180$	<0.001
Hypertension			$x^2=2.528$	0.112
Yes	15(30.6%)	11(17.7%)		
No	34(69.4%)	51(82.3%)		
Diabetes			$x^2=0.170$	0.680
Yes	6 (12.2%)	5 (8.1%)		
No	43(87.8%)	57(91.9%)		
Smoking			$x^2=0.567$	0.451
Yes	3 (6.1%)	1 (1.6%)		
No	46(93.9%)	61(98.4%)		
Hospital Stay (days)	15(12, 17)	14(13, 16)	$Z=-0.940$	0.347
Surgery Duration (minutes)	172.00(150.00, 217.50)	180.00(150.00, 230.00)	$Z=-0.062$	0.950
Intraoperative Blood Loss (ml)	300(175, 550)	200(100, 400)	$Z=-1.629$	0.103
BMI (kg/m^2)	23.44(20.81, 25.00)	23.10(22.80, 24.68)	$Z=-0.500$	0.617
Bone Density	-2.79 ± 0.83	-1.41 ± 0.87	$t=-8.441$	<0.001
Preoperative Farfan Index	59.92% ± 9.74%	58.01% ± 11.31%	$t=0.937$	0.351
Postoperative Farfan Index	66.69% ± 11.08%	67.29% ± 11.63%	$t=-0.274$	0.785
Adjusted Farfan Index	10.00%(5.25%, 14.05%)	8.70%(4.13%, 16.18%)	$Z=-0.264$	0.792
Surgical Segment/Case			$Z=-0.745$	0.456
L3-4	0 (0%)	1 (1.6%)		
L4-5	37(75.5%)	41(66.1%)		
L5-S1	12(24.5%)	20(32.3%)		
Anterior Vertebral Osteophyte			$Z=-2.796$	0.005
Grade 1	39(79.6%)	34(54.8%)		
Grade 2	8 (16.3%)	19(30.6%)		
Grade 3	2 (4.1%)	8 (12.9%)		
Grade 4	0 (0%)	1 (1.6%)		
Endplate Morphology			$Z=-2.768$	0.006
Flat Type	9 (18.4%)	26(41.9%)		
Concave Type	26(53.1%)	27(43.6%)		
Irregular Type	14(28.5%)	9 (14.5%)		
Lumbar CT Value	91.52 ± 39.52	151.46 ± 41.41	$t=-7.726$	<0.001
VBQ	3.20(2.78, 3.52)	2.84(2.46,3.07)	$Z=-3.549$	<0.001

Table 3 Results of the multivariate logistic regression model analysis for the cage subsidence group and Non-Cage subsidence group in the training set

Factor	B Value	SE Value	Wald Value	OR Value	95% CI	*P*-value
Age	0.029	0.044	0.446	1.030	0.945∼1.123	0.504
Bone Density	-1.589	0.502	10.013	0.204	0.076∼0.546	0.002
Anterior Vertebral Osteophyte	-	-	9.495	-	-	0.023
Grade 1	-	-	-	-	-	-
Grade 2	-1.506	0.779	3.736	0.222	0.048∼1.021	0.053
Grade 3	-4.015	1.391	8.333	0.018	0.001∼0.276	0.004
Grade 4	-20.245	40192.970	<0.001	<0.001	-	1.000
Endplate Morphology	-	-	1.644	-	-	0.440
Flat Type	-	-	-	-	-	-
Concave Type	0.967	0.756	1.634	2.629	0.597∼11.571	0.201
Irregular Type	0.554	0.832	0.443	1.740	0.340∼8.890	0.506
Lumbar CT Value	-0.030	0.012	5.822	0.971	0.947∼0.994	0.016
VBQ	-0.347	0.508	0.466	0.707	0.261∼1.914	0.495

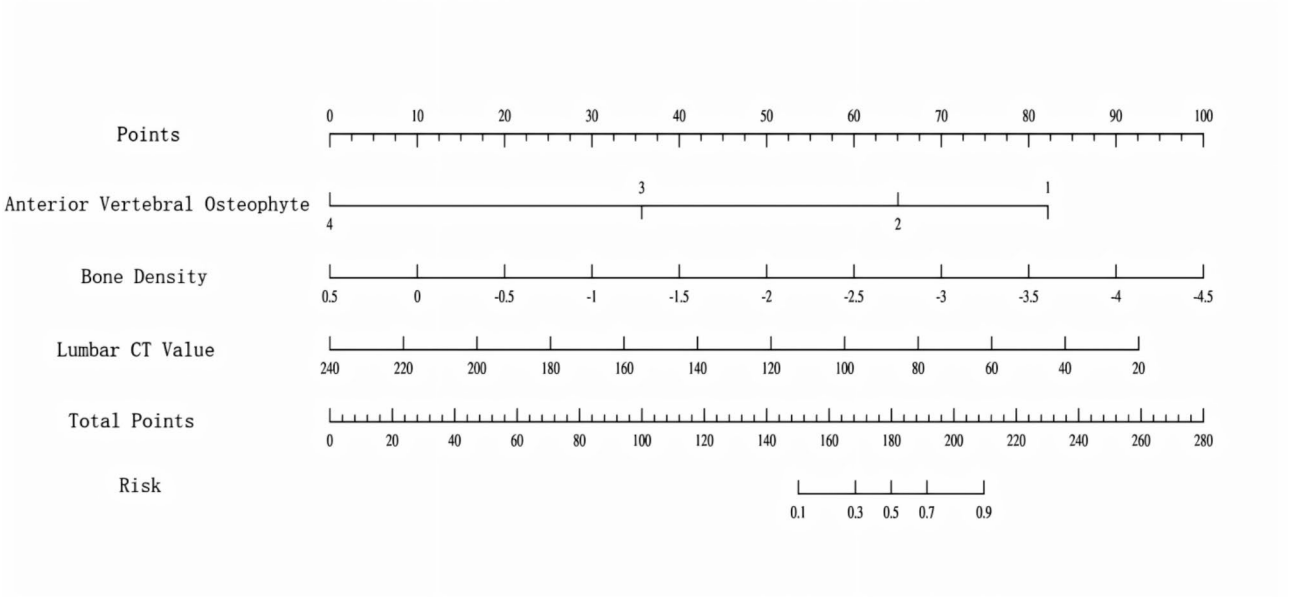

Fig. 6 nomogram of the risk of cage subsidence in patients after single-segment transforaminal lumbar interbody fusions

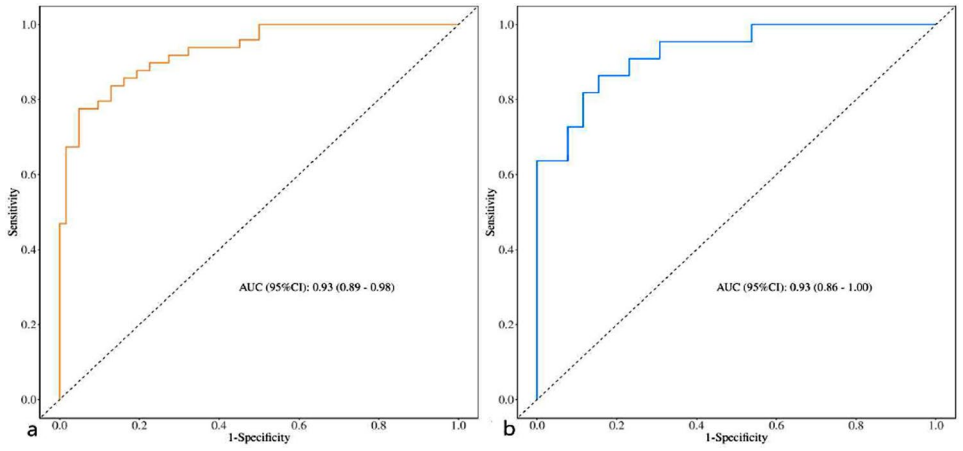

Fig. 7 ROC Curves for the Training Set and Validation Set (7a represents the ROC curve for the training set; 7b represents the ROC curve for the validation set)

than 0.7, suggesting that this patient has a high probability of experiencing interbody cage subsidence.

Model validation

The discrimination ability of the nomogram model was evaluated using the ROC curve. The results indicated that the AUC for the training set was 0.93 (95% CI 0.89–0.98) (see Fig. 7a), with specificity and sensitivity of 95% and 78%, respectively, yielding a Youden index of 0.73. In the validation set, the AUC was also 0.93 (95% CI 0.86–1.00) (see Fig. 7b), with specificity and sensitivity of 88% and 82%, respectively, resulting in a Youden index of 0.70. The calibration of the model was assessed using the Hosmer-Lemeshow goodness-of-fit test and calibration curves, revealing P-values of 0.616 for the training set and 0.904 for the validation set (both $P > 0.05$), indicating good consistency of the model (Fig. 8a and b). Additionally, decision curve analysis (DCA) was employed to evaluate the clinical utility of the model, demonstrating that the model's predictive risk threshold was substantial, and the use of the nomogram for predicting interventions in patients undergoing single-segment transforaminal lumbar interbody fusion yielded a high net benefit (see Fig. 9a and b).

Discussion

This study identified bone density, lumbar CT values, and anterior vertebral osteophytes as independent predictors of interbody cage subsidence following single-segment transforaminal lumbar interbody fusion, through both univariate and multivariate analyses. Previous research

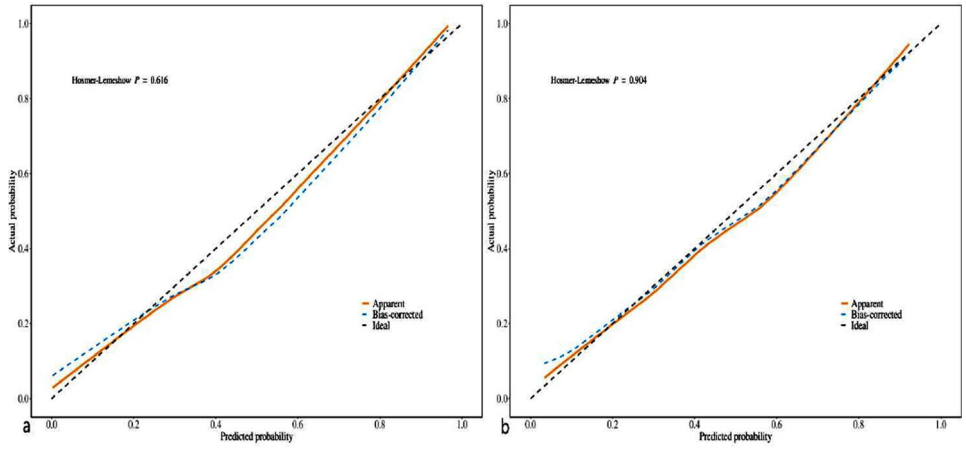

Fig. 8 Calibration curves for training and validation sets (8a is the training set calibration curve; 8b is the validation set calibration curve)

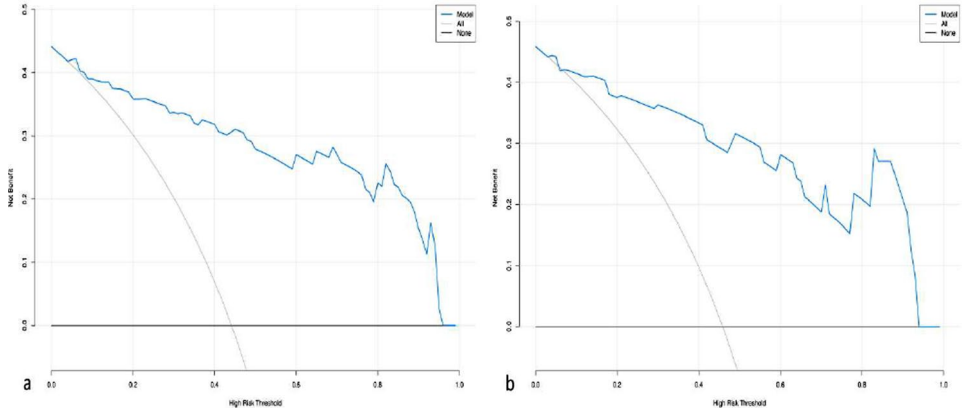

Fig. 9 Calibration curves for training and validation sets (9a is the training set calibration curve; 9b is the validation set calibration curve)

has indicated that a decrease in bone density significantly impairs postoperative bone healing capacity [21]. The presence of anterior vertebral osteophytes may indicate long-term degenerative changes, thereby affecting the mechanical properties of the vertebrae [22]. Additionally, lumbar CT values serve as an alternative indicator of bone quality, providing a direct reflection of the structural status of trabecular bone [23]. The findings of this study, when compared with existing literature, further confirm the critical role of bone density in postoperative complications following spinal surgery, while also revealing the potential value of anterior vertebral osteophytes and lumbar CT values as independent predictors [12, 24–26]. Although prior studies have emphasized the impact of bone density, this research is the first to include anterior vertebral osteophytes in the analysis, demonstrating their significant role in postoperative interbody cage subsidence. Furthermore, existing studies have shown that lumbar CT values are a reliable reference indicator in the clinical assessment of complications following spinal surgery [27–30].

As age increases, bone density typically declines, leading to a reduction in the strength and resilience of the skeleton, which makes the vertebrae more susceptible to subsidence under load [31]. Concurrently, osteoporosis is characterized by a decrease in bone mass and deterioration of the microstructure of bone tissue, further exacerbating skeletal fragility and reducing the stability of postoperative interbody fusion devices, thereby increasing the risk of subsidence [32]. The formation of anterior vertebral osteophytes occurs as the intervertebral disc, which serves as a cushioning structure between the vertebrae, gradually degenerates with age or prolonged stress, potentially leading to annular tears and disc herniation, which can compress surrounding tissues and trigger inflammation. Prolonged physical stress places continuous load on the anterior vertebrae, resulting in micro-damage and the formation of osteophytes [33, 34]. The inflammatory response promotes new bone formation, leading to local tissue proliferation and the development of osteophytes, which enhances stability and reduces the risk of interbody cage subsidence following lumbar surgery [35, 36]. CT values are important

indicators of vertebral bone density; generally, vertebrae with higher bone density can provide better load-bearing capacity, thereby more effectively supporting the fusion device and reducing the risk of subsidence. Conversely, low postoperative CT values may indicate insufficient bone density, leading to subsidence of the fusion device under load [30]. Relatively higher CT values are typically associated with better bone quality and a lower risk of subsidence. Considering these factors comprehensively aids in a deeper understanding of the risk of postoperative interbody cage subsidence, providing a more accurate basis for preoperative assessment in clinical practice.

Based on the aforementioned considerations, we constructed a nomogram model using preoperative bone density, anterior vertebral osteophytes, and lumbar CT values as predictive variables to assess the risk of interbody cage subsidence in patients undergoing single-segment transforaminal lumbar interbody fusion. This model is designed for clinical use, allowing physicians to input the various metrics of patients into the nomogram to calculate scores, thereby evaluating the probability of postoperative interbody cage subsidence. The predictive model demonstrated an AUC of 0.93 (95% CI 0.86–1.00) in the validation set, indicating superior diagnostic efficacy compared to previously established predictive models [13, 37, 38]. Additionally, the calibration of the model was assessed in both the training and validation sets using the Hosmer-Lemeshow goodness-of-fit test and calibration curves. The results indicated $P = 0.616$ for the training set and $P = 0.904$ for the validation set (both $P > 0.05$), suggesting that the model demonstrates good consistency. Furthermore, decision curve analysis (DCA) revealed a wide range of threshold values, indicating significant clinical applicability. It is noteworthy that the aforementioned indicators are both accessible and affordable, allowing for the effective utilization of available examination items in primary healthcare settings to assess the risk of interbody cage subsidence in patients following single-segment transforaminal lumbar interbody fusion.

Despite providing important insights into interbody cage subsidence following single-segment transforaminal lumbar interbody fusion, this study has several limitations. First, the small sample size may affect the generalizability and statistical power of the results, thereby limiting the ability to detect small effects. Second, the retrospective study design may introduce information bias, particularly during data collection and patient follow-up. Additionally, the relatively short follow-up period of the study did not allow for a comprehensive assessment of the occurrence of long-term complications and their impact on patient recovery. Finally, due to the limitations of this study, we are currently unable to perform external validation, which would further reinforce the clinical applicability of the predictive model.

Future research should focus on multiple directions to enhance the understanding and predictive capability regarding interbody cage subsidence following single-segment transforaminal lumbar interbody fusion. First, multicenter clinical trials are recommended to increase the sample size and enhance the generalizability of the results, while extending the follow-up period to better assess the impact of long-term complications. Second, adopting a prospective study design would help reduce information bias and ensure the accuracy and completeness of the data. Furthermore, an in-depth exploration of the biological mechanisms influencing cage subsidence, particularly through molecular biology and animal experiments to validate the effects of various factors, will provide a more scientific basis for clinical practice. Lastly, future studies could integrate other relevant risk factors to further refine the model and conduct external validation in independent cohorts to enhance its credibility, ensuring its effective application across various clinical settings.

In summary, this study conducted an in-depth analysis of the predictive value of bone density, lumbar CT values, and anterior vertebral osteophytes in relation to interbody cage subsidence following single-segment transforaminal lumbar interbody fusion. We developed a highly accurate nomogram predictive model to assess the risk of interbody cage subsidence in patients undergoing this procedure. This model not only provides clinicians with an effective preoperative assessment tool but also lays a solid foundation for formulating individualized treatment plans.

Acknowledgements
None.

Author contributions
JZ and QW contributed to conception and design of the study. WG and ZL drafted the manuscript. SC and QH processed the data and performed the analysis. DC provided valuable advice on the details in analysis and writing. All authors read and approved the final manuscript.

Funding
This work was supported by Key medical disciplines in Panyu District (2022–2024),Panyu District Science and Technology Programme Major Healthcare Projects (2022-Z04-112),Panyu District Science and Technology Program (2024-Z04-048) and Guangzhou Traditional Chinese Medicine and Integrated Traditional Chinese and Western Medicine Science and Technology Project(20222A010078).

Data availability
No datasets were generated or analysed during the current study.

Declarations

Ethics approval and consent to participate
This study was approved by the ethics committee of the Panyu Hospital of Chinese Medicine approved this study, which waived the requirement for individual consent due to the use of retrospective data.

Competing interests
The authors declare no competing interests.

Author details
[1]Department of Orthopedics, Panyu Hospital of Chinese Medicine, No. 65, Qiaodong Road, Shiqiao Street, Panyu District, Guangzhou, Guangdong 511400, China
[2]Guangzhou University of Chinese Medicine, Guangzhou, Guangdong 510006, China

Received: 11 December 2024 / Accepted: 12 March 2025
Published online: 21 April 2025

References

1. Donnally IC, Hanna A, Varacallo M. Lumbar degenerative disk disease (2024).
2. Iorio JA, Jakoi AM, Singla A. Biomechanics of degenerative spinal disorders. Asian Spine J. 2016;10(2):377–84. https://doi.org/10.4184/asj.2016.10.2.377.
3. Alentado VJ, Caldwell S, Gould HP, Steinmetz MP, Benzel EC, Mroz TE. Independent predictors of a clinically significant improvement after lumbar fusion surgery. Spine J. 2017;17(2):236–43. https://doi.org/10.1016/j.spinee.2016.09.011.
4. Chen E, Xu J, Yang S, Zhang Q, Yi H, Liang D, et al. Cage subsidence and fusion rate in extreme lateral interbody fusion with and without fixation. World Neurosurg. 2019;122:e969–77. https://doi.org/10.1016/j.wneu.2018.10.182.
5. Singhatanadgige W, Sukthuayat A, Tanaviriyachai T, Kongtharvonskul J, Tanasansomboon T, Kerr SJ, et al. Risk factors for polyetheretherketone cage subsidence following minimally invasive transforaminal lumbar interbody fusion. Acta Neurochir (Wien). 2021;163(9):2557–65. https://doi.org/10.1007/s00701-021-04923-y.
6. Zavras AG, Federico V, Nolte MT, Butler AJ, Dandu N, Munim M, et al. Risk factors for subsidence following anterior lumbar interbody fusion. Global Spine J. 2024;14(1):257–64. https://doi.org/10.1177/21925682221103588.
7. Davis TT, Hynes RA, Fung DA, Spann SW, MacMillan M, Kwon B, et al. Retroperitoneal oblique corridor to the l2-s1 intervertebral discs in the lateral position: an anatomic study. J Neurosurg Spine. 2014;21(5):785–93. https://doi.org/10.3171/2014.7.SPINE13564.
8. Tempel ZJ, McDowell MM, Panczykowski DM, Gandhoke GS, Hamilton DK, Okonkwo DO, et al. Graft subsidence as a predictor of revision surgery following stand-alone lateral lumbar interbody fusion. J Neurosurg Spine. 2018;28(1):50–6. https://doi.org/10.3171/2017.5.SPINE16427.
9. Kotheeranurak V, Jitpakdee K, Lin GX, Mahatthanatrakul A, Singhatanadgige W, Limthongkul W, et al. Subsidence of interbody cage following oblique lateral interbody fusion: an analysis and potential risk factors. Global Spine J. 2023;13(7):1981–91. https://doi.org/10.1177/21925682211067210.
10. Amorim-Barbosa T, Pereira C, Catelas D, Rodrigues C, Costa P, Rodrigues-Pinto R, et al. Risk factors for cage subsidence and clinical outcomes after transforaminal and posterior lumbar interbody fusion. Eur J Orthop Surg Traumatol. 2022;32(7):1291–99. https://doi.org/10.1007/s00590-021-03103-z.
11. Park MK, Kim KT, Bang WS, Cho DC, Sung JK, Lee YS, et al. Risk factors for cage migration and cage retropulsion following transforaminal lumbar interbody fusion. Spine J. 2019;19(3):437–47. https://doi.org/10.1016/j.spinee.2018.08.007.
12. Jones C, Okano I, Salzmann SN, Reisener MJ, Chiapparelli E, Shue J, et al. Endplate volumetric bone mineral density is a predictor for cage subsidence following lateral lumbar interbody fusion: a risk factor analysis. Spine J. 2021;21(10):1729–37. https://doi.org/10.1016/j.spinee.2021.02.021.
13. Pu X, Wang X, Ran L, Xie T, Li Z, Yang Z, et al. Comparison of predictive performance for cage subsidence between ct-based Hounsfield units and mri-based vertebral bone quality score following oblique lumbar interbody fusion. Eur Radiol. 2023;33(12):8637–44. https://doi.org/10.1007/s00330-023-09929-x.
14. Chen Q, Ai Y, Huang Y, Li Q, Wang J, Ding H, et al. Mri-based endplate bone quality score independently predicts cage subsidence following transforaminal lumbar interbody fusion. Spine J. 2023;23(11):1652–58. https://doi.org/10.1016/j.spinee.2023.07.002.
15. Pappou IP, Cammisa FJ, Girardi FP. Correlation of end plate shape on mri and disc degeneration in surgically treated patients with degenerative disc disease and herniated nucleus pulposus. Spine J. 2007;7(1):32–8. https://doi.org/10.1016/j.spinee.2006.02.029.
16. Chen H, Zhong J, Tan J, Wu D, Jiang D. Sagittal geometry of the middle and lower cervical endplates. Eur Spine J. 2013;22(7):1570–75. https://doi.org/10.1007/s00586-013-2791-8.
17. Nathan H. Compression of the sympathetic trunk by osteophytes of the vertebral column in the abdomen: an anatomical study with pathological and clinical considerations. Surgery. 1968;63(4):609–25.
18. Imagama S, Ando K, Kobayashi K, Machino M, Tanaka S, Morozumi M, et al. Impact of pelvic incidence on lumbar osteophyte formation and disc degeneration in middle-aged and elderly people in a prospective cross-sectional cohort. Eur Spine J. 2020;29(9):2262–71. https://doi.org/10.1007/s00586-019-06204-w.
19. Zhou Jing Z, Lei L, Chao Y, Chao W. Vertebral body Ct values to predict fusion subsidence after simple oblique lateral lumbar interbody fusion. Chin J Repair Reconstr Surg. 2021;35(11):1449–56.
20. Hu YH, Yeh YC, Niu CC, Hsieh MK, Tsai TT, Chen WJ, et al. Novel mri-based vertebral bone quality score as a predictor of cage subsidence following transforaminal lumbar interbody fusion. J Neurosurg Spine. 2022;37(5):654–62. https://doi.org/10.3171/2022.3.SPINE211489.
21. He Z, Sun C, Ma Y, Chen X, Wang Y, Chen K, et al. Rejuvenating aged bone repair through multihierarchy reactive oxygen species-regulated hydrogel. Adv Mater. 2024;36(9):e2306552. https://doi.org/10.1002/adma.202306552.
22. Li Chuanling Z, Feng L, Huizhao X, Feipeng Z. Changes of vertebral sclerosis and osteophytes after lumbar fusion. J Practical Orthop. 2016;22(12):1087–90. https://doi.org/10.13795/j.cnki.sgkz.2016.12.009.
23. Chen Xuanhuang Z, Min Z, Wenhua GH, Xu C, Zhengxi Y, et al. Quality control of Ct values in bone scanned using thin-layer Ct. Chin J Osteoporos. 2017;23(12):1546–50.
24. Schwaiger BJ, Gersing AS, Baum T, Noel PB, Zimmer C, Bauer JS. Bone mineral density values derived from routine lumbar spine multidetector row Ct predict osteoporotic vertebral fractures and screw loosening. Ajnr Am J Neuroradiol. 2014;35(8):1628–33. https://doi.org/10.3174/ajnr.A3893.
25. Yuan C, Zhou J, Wang L, Deng Z. Adjacent segment disease after minimally invasive transforaminal lumbar interbody fusion for degenerative lumbar diseases: incidence and risk factors. Bmc Musculoskelet Disord. 2022;23(1):982. https://doi.org/10.1186/s12891-022-05905-6.
26. Chen Q, Tu Z, Ai Y, Li W, Chen J, Feng J, et al. Forearm bone mineral density predicts screw loosening after lumbar fusion similar to lumbar Hounsfield unit value in patients with lumbar spondylolisthesis. Osteoporos Int. 2024;35(3):543–49. https://doi.org/10.1007/s00198-023-06957-7.
27. De Stefano F, Elarjani T, Warner T, Lopez J, Shah S, Basil GW, et al. Hounsfield unit as a predictor of adjacent-level disease in lumbar interbody fusion surgery. Neurosurgery. 2022;91(1):146–49. https://doi.org/10.1227/neu.0000000000001949.
28. Li J, Zhang Z, Xie T, Song Z, Song Y, Zeng J. The preoperative Hounsfield unit value at the position of the future screw insertion is a better predictor of screw loosening than other methods. Eur Radiol. 2023;33(3):1526–36. https://doi.org/10.1007/s00330-022-09157-9.
29. Wu H, Cheung J, Zhang T, Shan Z, Zhang X, Liu J, et al. The role of Hounsfield unit in intraoperative endplate violation and delayed cage subsidence with oblique lateral interbody fusion. Global Spine J. 2023;13(7):1829–39. https://doi.org/10.1177/21925682211052515.
30. Zhou J, Yuan C, Liu C, Zhou L, Wang J. Hounsfield unit value on Ct as a predictor of cage subsidence following stand-alone oblique lumbar interbody fusion for the treatment of degenerative lumbar diseases. Bmc Musculoskelet Disord. 2021;22(1):960. https://doi.org/10.1186/s12891-021-04833-1.
31. Farr JN, Fraser DG, Wang H, Jaehn K, Ogrodnik MB, Weivoda MM, et al. Identification of senescent cells in the bone microenvironment. J Bone Min Res. 2016;31(11):1920–29. https://doi.org/10.1002/jbmr.2892.
32. Specialized Committee on Prevention and Control of Spinal Diseases of Chinese Preventive Medical Association, Specialized Committee on Prevention and Rehabilitation of Osteoporosis of Chinese Society of Rehabilitation Medicine. Guidelines for the prevention of osteoporosis-related complications in patients undergoing lumbar fusion and internal fixation (2024). Chin J Bone Joint Surg. 2024;17(05):389–403.
33. Liang R, Lu Changwei W, Yihua. Advances in Biomechanical research on lumbar intervertebral disc degeneration and injury. Electron J Clin Med Literature. 2018;5(48):198. https://doi.org/10.16281/j.cnki.jocml.2018.48.171.
34. Ma Zheng. Relationship between Modic changes and intervertebral disc height and vertebral osteophytes [M.S.], Hebei Medical University. 2013;.
35. Klaassen Z, Tubbs RS, Apaydin N, Hage R, Jordan R, Loukas M. Vertebral spinal osteophytes. Anat Sci Int. 2011;86(1):1–09. https://doi.org/10.1007/s12565-010-0080-8.

36. Fan YC, Cai DL, Guo WJ, Liao PJ, Wei QP. Influence of lumbar endplate morphology on fusion settling after transforaminal lumbar interbody fusion. J Practical Orthop. 2023;29(03):193–97. https://doi.org/10.13795/j.cnki.sgkz.2023.03.008.
37. Xie F, Yang Z, Tu Z, Huang P, Wang Z, Luo Z, et al. The value of Hounsfield units in predicting cage subsidence after transforaminal lumbar interbody fusion. Bmc Musculoskelet Disord. 2022;23(1):882. https://doi.org/10.1186/s12891-022-05836-2.
38. Ran L, Xie T, Zhao L, Wang C, Luo C, Wu D, et al. Mri-based endplate bone quality score predicts cage subsidence following oblique lumbar interbody fusion. Spine J. 2024;24(10):1922–28. https://doi.org/10.1016/j.spinee.2024.05.002.

Publisher's note